STUDY ON KINETICS AND ISOTHERMS OF RHODAMINE B ADSORPTION ON SOLVOTHERMAL SYNTHESIZED MIL-53(Al)

Pham Dinh Du[(1)]

(1) Thu Dau Mot University
Corresponding author: dupd@tdmu.edu.vn

DOI: 10.37550/tdmu.EJS/2024.02.548

Article Info

Volume: 6
Issue: 02
June 2024
Received: Mar. 15th, 2024
Accepted: April 22nd, 2024
Page No: 214-219

Abstract

In this paper, MIL-53(Al) was synthesized by solvothermal method and its application as an adsorbent to remove rhodamine B from aqueous solution. The material was characterized using X-ray diffraction, Fourier-transform infrared spectroscopy, nitrogen adsorption-desorption isotherms, and scanning electron microscopy. The results show that the material has a large specific surface area (1028.3 m2/g). The rhodamine B adsorption on MIL-53(Al) occurs very quickly in the first minutes of contact. Two pseudo-first order and pseudo-second order adsorption kinetic models, and two adsorption isotherm models, including Langmuir and Freundlich, were used to analyze the adsorption data.

Keywords: adsorption, isotherm, kinetic, MIL-53(Al), rhodamine B

1. Introduction

Dyes are widely used in numerous applications, such as textile, paper, plastic, and dye industries (Dai et al., 2021). The amount of dyes produced annually worldwide is estimated at over 7×10^5 tons, and more than 100,000 commercially available dyes with different physical and chemical properties are being used (Allen et al., 2004; Al-Qodah et al., 2007). Various dyes and their decomposition products are toxic and carcinogenic, thus posing a danger to aquatic organisms (Dai et al., 2021; Eftekhari et al., 2010). Therefore, dye removal from wastewater is essential. Rhodamine B (RB) is an important representative of xanthene dyes, widely used as a colorant in textiles and foods, and is also a famous fluorescent water marker. RB has carcinogenic properties, reproductive and developmental toxicity, neurotoxicity and chronic toxicity to humans and animals. RB is a typical persistent organic dye contaminant and is often chosen as a representative pollutant to evaluate the adsorption-catalytic ability of materials (Chen et al., 2012).

Many different techniques have been used to remove dyes from aqueous solutions. Among them, adsorption is considered a suitable technique because of its simplicity and effectiveness (Eftekhari et al., 2010). MIL-53(Al) is a metal-organic framework material with a large specific surface area (Patil et al., 2011; Loiseau et al., 2004), high hydrogen storage capacity (Férey et al., 2003), as well as the ability to be used as a catalyst, adsorption, separation, and gas storage (Patil et al., 2011; Du et al., 2011; Rahmani & Rahmani, 2018; Malsche et al., 2012). In this study, MIL-53(Al) was synthesized by solvothermal method and applied as an adsorbent to remove RB from aqueous solution. The kinetics and isotherms of the adsorption process were analyzed.

2. Experimental

2.1. Material synthesis

The synthesis of MIL-53(Al) was adapted from previous papers (Du et al., 2011; Rahmani & Rahmani, 2018; Loiseau et al., 2004). A mixture of aluminium (III) chloride (14.685g), terephthalic acid (9.13g) and N'N-dimethylformamide (180mL) was placed in a Teflon-lined steel autoclave (200mL) and put to an oven for 3 days at 120ºC. Then, the solid product was filtered, washed with methanol, and dried overnight at 100°C to get MIL-53(Al).

The materials were characterized with scanning electron microscopy (SEM) (SEM JMS-5300LV, Japan), X-ray diffraction (XRD) (VNU-D8 Advance, Bruker, Germany), Fourier-transform infrared spectroscopy (FT-IR) (Jasco FT/IR-4600, Japan), and nitrogen adsorption measurements (Micromeritics, Tristar 3000). The textural properties of the material were examined via the surface area and porosity after a heat treatment at 200°C with N_2 for 5 h. The concentration of RB solution was determined with the UV-Vis method on a Jasco V-770 (Japan) at λ_{max} = 554nm.

2.2. Adsorption experiments

MIL-53(Al) (0.1g) was placed into a double-necked flask containing 100mL of RB solution with the concentration in the range of 5-25mg/L under magnetic stirring at ambient temperature (29 ± 2°C). At a specified interval, a definite volume of solution was withdrawn, filter to remove the adsorbent, and the concentration of RB was determined.

The adsorption capacity at time *t* (q_t) and equilibrium (q_e) were calculated according to Eqs. 1 and 2.

$$q_t = \frac{(C_0 - C_t) \times V}{m} \quad (1)$$

$$q_e = \frac{(C_0 - C_e) \times V}{m} \quad (2)$$

where C_0, C_t, and C_e (mg/L) are the concentration of RB in the solution at the beginning, *t*, and equilibrium; *V* (L) is the volume of RB solution; *m* (g) is the weight of the dry adsorbent.

3. Results and discussion

3.1. Characteristic properties of the material

The XRD pattern appears diffraction peaks at 9.1, 10.2, 15.3, 18.3, 20.9, 25.5 and 27.6º (Fig. 1a), and they are characteristic for MIL-53(Al) (Moran et al., 2018; Rahmani & Rahmani, 2018; Liu et al., 2019; Rallapalli et al., 2010). These peaks are indexed according to the simulated XRD pattern of MIL-53*as* (Al) from the CCDC220475 database. This proves that the MIL-53(Al) structure has been formed. In addition, the diffraction peaks of Al does not appear on the pattern, probably because Al exists in single-atom form.

The FT-IR spectra of MIL-53(Al) is presented in Fig. 1b. The absorption bands at 1616 and 1509cm^{-1} correspond to the asymmetric stretching vibration of –COO group, while the absorption band at 1416 corresponds to the symmetric stretching vibration of –COO group (Patil et al., 2011; Liu et al., 2019; Loiseau et al., 2004). The absorption peak observed at 1700cm^{-1} ($\nu_{C=O}$) can be attributed to free terephthalic acid molecules attached within the pores in their protonated form (–CO_2H) (Loiseau et al., 2004). The peaks in the low wavenumber region (479–594 cm^{-1}) are due to the presence of Al–O in MIL-53(Al) (Liu et al., 2019). The absorption bands located in the region 3600–2500cm^{-1} are characteristic for the freely adsorbed water, as well as the stretching vibration of the OH groups in –COOH and Al–OH fragments (Isaeva et al., 2019). These values confirm the existence of CO_2^- group covalently bonded to aluminium within the material.

The isotherms of MIL-53(Al) belong to type I with the condensation at relatively low pressure (Fig. 1c), indicating that the material has porosity at a micron scale (Leofanti et al., 1998). The specific

surface area of MIL-53(Al) sample is 1028.3m^2/g, similar to some other publications about this material (Patil et al., 2011; Loiseau et al., 2004). Here, the sample treatment before measurement (with N_2 at 200°C) may have opened up the micropores in the material structure. The pore size distribution curve of MIL-53(Al) sample shows that the material has pores with a size of about 3.9nm (insert in Fig. 1c). Figure 1d shows that the MIL-53(Al) has a shape resembling rice grains with a length of about 0.3µm.

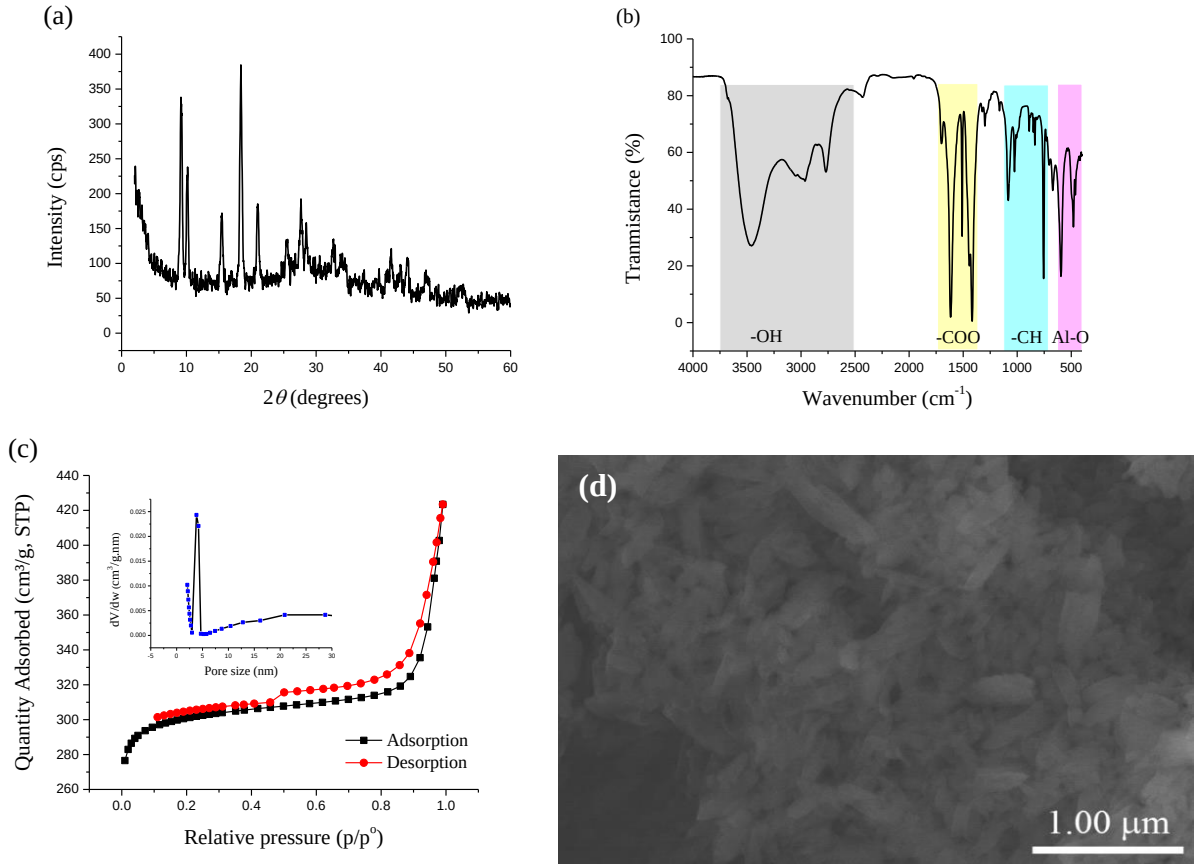

Figure 1. XRD pattern (a), FT-IR spectra (b), nitrogen adsorption-desorption isotherms and pore size distribution (c), and SEM image (d) of the MIL-53(Al) sample

3.2. Adsorption studies

3.2.1. Effect of initial concentration and contact time

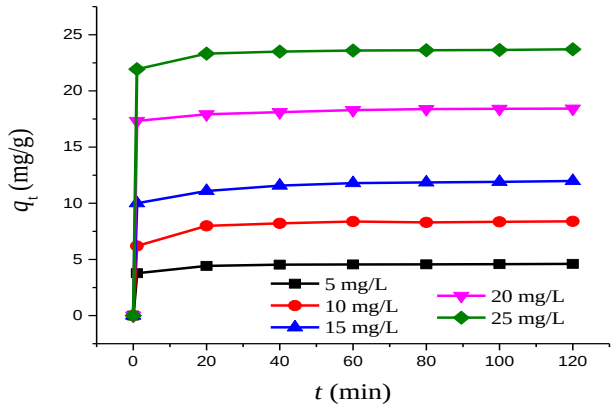

Figure 2. *RB adsorption capacity on MIL-53(Al)*

We can see that the adsorption capacity of RB increases with the increase of the initial concentration (Fig. 2). This difference probably depends on the concentration difference of the number of RB on the adsorbent surface and in the solution (driving force). When the initial concentration is small, the

driving force is also small, leading to low adsorption capacity. The adsorption capacity increases with the driving force, but this increase becomes smaller when the initial concentration is higher. Figure 2 also shows that the RB adsorption occurs very rapidly during the first min of contact, then it decreases slowly during the next 40 min and becomes stable after 120 min. Thus, the time required for the adsorption of RB on MIL-53(Al) to reach the adsorption-desorption equilibrium is 40 min.

3.2.2. Adsorption kinetics

Chemical kinetics is indispensable in adsorption studies to determine the adsorption rate of the adsorbate at the solid interface. Kinetic models allow estimation of adsorption rates and lead to suitable rate expressions and characterization of the possible reaction mechanisms. Two kinetic models, namely pseudo-first order and pseudo-second order, are commonly used to test experimental data, are Eqs. 3 and 4 (Patil et al., 2011).

$$\ln(q_e - q_t) = \ln q_1 - k_1 \times t \quad (3)$$

$$\frac{t}{q_t} = \frac{1}{k_2 \times q_2^2} + \frac{1}{q_2} \times t \quad (4)$$

where k_1 (min^{-1}) and k_2 (g/mg·min) are the rate constants for the pseudo-first order and the pseudo-second order adsorption kinetics; q_1 and q_2 (mg/g) are the corresponding maximum adsorption capacities.

The $\ln(q_e - q_t) = f(t)$ plot describes pseudo-first order kinetics, and the $t/q_t = f(t)$ plot describes pseudo-second order kinetics (Fig. 3 and Table 1). Figure 3 shows that the experimental data follow the pseudo-second order equation better because the data points lie closer to the theoretical line $R^2 > 0.9998$ (Table 1). Furthermore, the equilibrium adsorption capacity values, q_2, calculated from the pseudo-second order equation is very close to the experimental equilibrium adsorption capacity values, q_e. This also proves that the RB adsorption on MIL-53(Al) obeys the adsorption kinetic model of pseudo-second order. Therefore, it can be assumed that RB adsorption is controlled by chemisorption, which involves valence forces through the sharing or exchange of electrons between the adsorbent and the adsorbate (Shao et al., 2014).

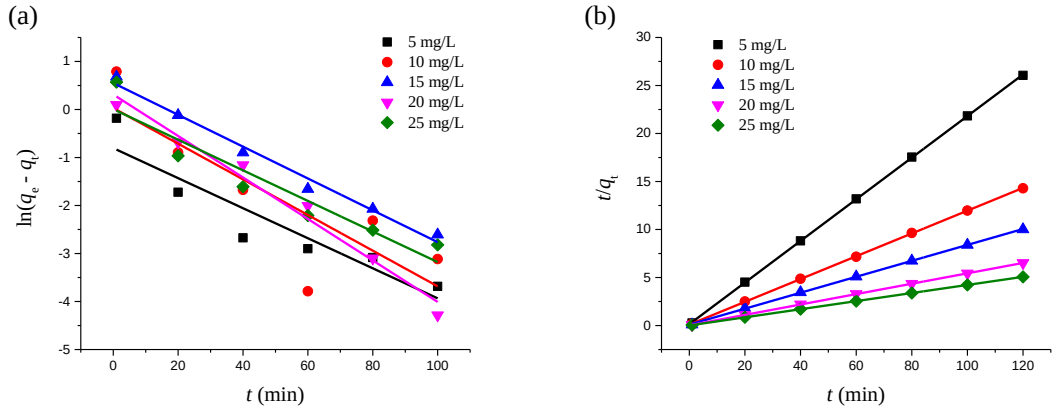

Figure 3. *Corresponding linear fitting curves via the pseudo-first order (a) the pseudo-second order (b) kinetic models*

TABLE 1. The comparison of kinetic parameters for RB adsorption on MIL-53(Al) at the different initial concentration

Initial RB concentration (mg/g)	q_e (mg/g)	Pseudo-first order			Pseudo-second order		
		k_1 (min^{-1})	q_1 (mg/g)	R^2	k_2 (g/mg·min)	q_2 (mg/g)	R^2
5	4.6	0.0313	0.4	0.8650	0.3386	4.6	1.0000
10	8.4	0.0371	1.0	0.7068	0.1512	8.4	0.9999
15	12.0	0.0332	1.7	0.9851	0.0718	12.0	0.9998
20	18.4	0.0432	1.4	0.9797	0.1139	18.5	1.0000
25	23.7	0.0319	1.0	0.8971	0.1549	23.7	1.0000

3.2.3. Adsorption isotherms

The study of adsorption isotherms is critical in describing the characteristic relationship between the concentration of the adsorbate and the adsorption capacity of the adsorbent, especially when designing an ideal adsorption system in industry (Shao et al., 2014). To investigate the adsorption of RB onto MIL-53(Al), we use the Freundlich and Langmuir models to analyze the data (Eqs. 5 and 6).

$$\ln q_e = \ln K_F + \frac{1}{n} \times \ln C_e \quad (5)$$

$$\frac{C_e}{q_e} = \frac{1}{q_m} \times C_e + \frac{1}{K_L \times q_m} \quad (6)$$

where K_F is the Freundlich constant ($mg^{(1-1/n)} \cdot L^{1/n} \cdot g^{-1}$), and n is the adsorption intensity; K_L constant is related to the adsorption energy (L/g), and q_m is the Langmuir monolayer adsorption capacity (mg/g).

From Fig. 4, we can see that both the Langmuir and Freundlich models do not describe the experimental data well, the experimental points are far from the regression line. This indicates that the RB adsorption on MIL-53(Al) is quite complicatedly. Table 2 shows that the Langmuir model has a higher correlation coefficient (R^2 = 0.6292) than the Freundlich model (R^2 = 0.3549), indicating that the former is more suitable than the latter for the data. The maximum capacity of monolayer adsorption is 14.2mg/g. The value is higher than what was obtained by silica extracted from rice husk (6–6.87mg/g) (Tsamo et al., 2020) and amino acid functionalized Fe_3O_4 nanoparticles (10.44mg/g) (Belachew et al., 2021).

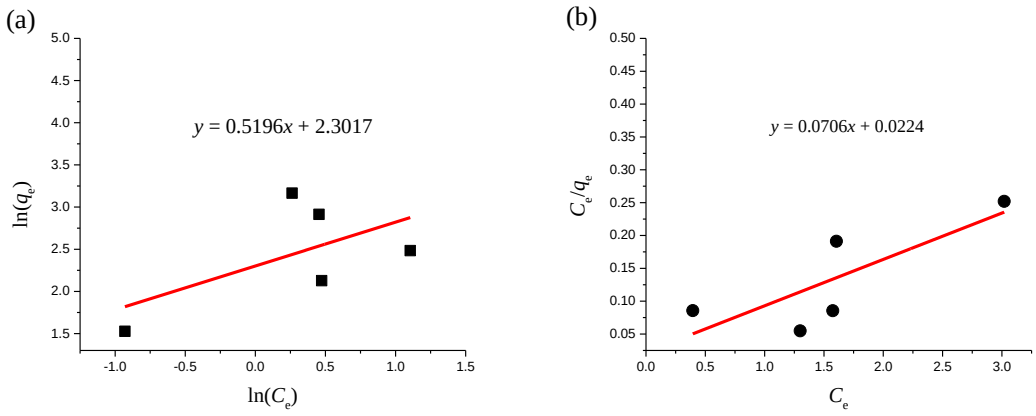

Figure 4. Corresponding linear fitting curves of Freundlich (a) and Langmuir (b) models

TABLE 2. Regression parameters of isothermal models of RB adsorption on MIL-53(Al)

Parameter	Model	
	Freundlich	Langmuir
K_F ($mg^{(1-1/n)} \cdot L^{1/n} \cdot g^{-1}$)	0.834	–
n	1.92	–
K_L (L/g)	–	3.152
q_m (mg/g)	–	14.2
R^2	0.3549	0.6292

4. Conclusions

The resulting MIL-53(Al) has a large specific surface area (S_{BET} = 1028.3m^2/g) and high crystallinity. The morphology of the material resembles rice grains with a size of about 0.3µm. The rhodamine B adsorption on MIL-53(Al) follows the pseudo-second order adsorption kinetic model. The adsorption occurs rapidly during the first minutes of contact and reaches adsorption-desorption equilibrium after 40 minutes. The Langmuir adsorption isotherm model is more suitable to describe the adsorption process than the Freundlich isotherm model. The maximum adsorption capacity determined from the Langmuir isotherm model is 14.2mg/g. The material is a potential adsorbent in the treatment of water contaminated with organic dyes.

Acknowledgments

This research is funded by Thu Dau Mot University under grant number DT.22.2-006.

References

Al-Qodah, Z., et al. (2007). Adsorption of methylene blue by acid and heat treated diatomaceous silica. *Desalination*, vol. 217, pp. 212-224. https://doi.org/10.1016/j.desal.2007.03.003

Allen, S. J., et al. (2004). Adsorption isotherm models for basic dye adsorption by peat in single and binary component systems. *Journal of Colloid and Interface Science*, *280*(2), 322-333. https://doi.org/10.1016/j.jcis.2004.08.078

Belachew, N., et al. (2021). Synthesis of amino acid functionalized Fe_3O_4 nanoparticles for adsorptive removal of rhodamine B. *Applied Water Science*, *11*(2), 33, 2021. https://doi.org/10.1007/s13201-021-01371-y

Chen, X., et al. (2012). Oxidation Degradation of Rhodamine B in Aqueous by UV/$S_2O_8^{2-}$ Treatment System. *Hindawi International Journal of Photoenergy*, Article ID 754691. https://doi.org/10.1155/2012/754691

Dai, D., et al. (2021). Mn-doped Fe_2O_3/diatomite granular composite as an efficient Fenton catalyst for rapid degradation of an organic dye in solution. *Journal of Sol-Gel Science and Technology*, *97*(2), pp. 329-339. https://doi.org/10/1007/s10971-020-05452-3

Du, J. J., et al. (2011). New photocatalysts based on MIL-53 metal-organic frameworks for the decolorization of methylene blue dye. *Journal of Hazardous Materials*, 190, pp. 945-951. https://doi.org/10.1016/j.jhazmat.2011.04.029

Eftekhari, S., et al. (2010). Application of AlMCM-41 for competitive adsorption of methylene blue and rhodamine B: thermodynamic and kinetic studies. *Journal of Hazardous Materials*, *178*(1-3), pp. 349-355. https://doi.org/10.1016/j.jhazmat.2010.01.086

Férey, G., et al. (2003). Hydrogen adsorption in the nanoporous metal-benzenedicarboxylate M(OH)(O_2C–C_6H_4–CO_2) (M = Al^{3+}, Cr^{3+}), MIL-53. *Chem. Commun*, 37, pp. 2976-2977. https://doi.org/10.1039/B308903G

Isaeva, V. I., et al. (2019). Adsorption of 2,4-dichlorophenoxyacetic acid in an aqueous medium on nanoscale MIL-53(Al) type materials. *Dalton Trans.*, 48, pp. 15091-15104. https://doi.org/10.1039/C9DT03037A

Leofanti, G., et al. (1998). Surface area and pore texture of catalysts. *Catalysis Today*, 41, pp. 207-219. https://doi.org/10.1016/S0920-5861(98)00050-9

Liu, J. F., et al. (2019). Pd nanoparticles immobilized on MIL-53(Al) as highly effective bifunctional catalysts for oxidation of liquid methanol to methyl formate. *Petroleum Science*, 16, pp. 901-911. https://doi.org/10.1007/s12182-019-0334-6

Loiseau, T., et al. (2004). A Rationale for the Large Breathing of the Porous Aluminum Terephthalate (MIL-53) Upon Hydration. *Chem. Eur. J*, 10, pp. 1373-1382. https://doi.org/10.1002/chem.200305413

Malsche, W. D., et al. (2012). Unusual pressure-temperature dependency in the capillary liquid chromatographic separation of C8 alkylaromatics on the MIL-53(Al) metal-organic framework. *Micropor. Mesopor. Mat*, 162, pp. 1-5. https://doi.org/10.1016/j.micromeso.2012.06.002

Moran, C. M., et al. (2018). Structured Growth of Metal-Organic Framework MIL-53(Al) from Solid Alumium Carbide Precursor. *J. Am. Chem. Soc*, *140*(29), pp. 9148-9153. https://doi.org/10.1021/jacs.8b04369

Patil, D. V., et al. (2011). MIL-53(Al): An Efficient Adsorbent for the Removal of Nitrobenzene from Aqueous Solutions. *Ind. Eng. Chem. Res*, 50, pp. 10516-10524. https://doi.org/10.1021/ie200429f

Rahmani, E., & Rahmani, M. (2018). Al-based MIL-53 Metal Organic Framework (MOF) as the New Catalyst for Friedel-Crafts Alkylation of Benzene. *Ind. Eng. Chem. Res*, *57*(1), pp. 169-178. https://doi.org/10.1021/acs.iecr.7b04206

Rallapalli, P., et al. (2010). An alternative activation method for the enhancement of methane storage capacity of nanoporous aluminium terephthalate, MIL-53(Al). *J. Porous Mater*, 17, pp. 523-528. https://doi.org/10.1007/s10934-009-9320-5

Shao, Y., et al. (2014). Application of Mn/MCM-41 as an adsorbent to remove methyl blue from aqueous solution. *Journal of Colloid and Interface Science*, vol. 429, pp. 25-33. https://doi.org/10.1016/j.jcis.2014.05.004

Tsamo, C., et al. (2020). Removal of rhodamine B from aqueous solution using silica extracted from rice husk. *SN Applied Science*, *2*(2), pp. 256. https://doi.org/10.1007/s42452-020-2057-0.